Roles of GALACTURONOSYLTRANSFERASES in Arabidopsis development

by

Allison Rachel Triebe

A thesis submitted to the graduate faculty

in partial fulfillment of the requirements for the degree of

MASTER OF SCIENCE

Major: Genetics and Genomics

Program of Study Committee:
Dior R. Kelley, Major Professor
Olga A. Zabotina
Hongqing Guo

The student author, whose presentation of the scholarship herein was approved by the program of study committee, is solely responsible for the content of this thesis. The Graduate College will ensure this thesis is globally accessible and will not permit alterations after a degree is conferred.

Iowa State University
Ames, Iowa
2024

DEDICATION

To my parents for their constant love and support throughout my life. As well as all the science teachers throughout my schooling that have nurtured my love of science and all the advice and help, they have given me.

TABLE OF CONTENTS

LIST OF FIGURES

LIST OF TABLES

NOMENCLATURE

ABP1	Auxin binding protein 1
ARF	Auxin response factor
AI	Artificial intelligence
AT	Aminotransferase
BLR	BELLRINGER
BiFC	Bimolecular Fluorescence Complementation assay
BR	Brassinosteroid
CSC	Cellulose synthase complexes
CWM	Cell wall mutant
DAMPS	Danger-associated molecular patterns
ELISA	Enzyme-linked immunosorbent assay
ELMO	Engulfment and cell motility
FTIR	Fourier transform infrared (FTIR) micro spectroscopy
GAUT	Galaturonosyltransferase
GalAT	α-1,4-galacturonosyltransferase
HG	Homogalacturonan
IAA	Indole-3-acetic acid
IAM	Indole-3-acetamide
IAOx	Indole-3-acetaldoxime
ING	Indole-3-glycerol phosphate
IND	Indole
IPyA	Indole-3pyruvic acid
LS	Linsmaier and Skoog media

LRD	Lateral Root Density
ML	Machine learning
MLGs	Mixed-linkage glucans
NAA	Naphthaleneacetic acid
NPA	N-1-naphthylphthalamic acid
PCR	Polymerase chain reaction
PME	Pectin methyl-esterase
PMEI	Pectin methyl-esterase inhibitor
PMT	Pectin methyltransferase
Pi	Inorganic phosphorus
QUA1	Quasimodo 1
RAM	Root Apical Meristem
RG-1	Rhamnogalacturonan I
RG-2	Rhamnogalacturonan II
SAM	Shoot apical meristem
SEM	Scanning electron microscope
TAA	Tryptophan aminotransferase of Arabidopsis
TAM	Tryptamine
TARs	TAA1-related proteins
TMK	Transmembrane Domain Kinase
TPL	TOPLESS
Trp	Tryptophan
XG	Xylogalacturonan
XyG	Xyloglucans
WT	Wild Type

ACKNOWLEDGMENTS

I would like to thank my advisor, Dr. Dior Kelley, for her support and mentorship this last couple of years. As well as the support of my committee member, Dr. Olga Zabotina and Dr. Hongqing Guo for their advice and support. I know without their guidance and support I would not be where I am now. I would also like to thank all my lab members and (current and former) undergraduates that have helped me through so much and given me a great deal of advice on my research.

Finally, I would like to acknowledge the funding that has supported my research, this work was supported by National Science Foundation Award No. 2118253 to Dior Kelley and Olga Zabotina. I was also supported by NSF Award No. 2152117, Dependable Data Driven Discovery NSF Research Traineeship.

ABSTRACT

Plant cells are encapsulated by cell walls that provide critical surface protection and cellular structure. Cell walls are dynamically regulated during plant development through the activity of cell wall modifying enzymes. However, how cell wall composition is modulated in roots to influence organogenesis is not well understood. In Arabidopsis, the pectin synthesis enzyme GALACTURONOSYLTRANSFERASE10 (GAUT10) has been shown to be required for both root elongation and cell division in primary roots, leading to a short root phenotype in the absence of *GAUT10*. GAUT proteins can form complexes and may work in concert with one another to influence cell wall composition. Gene expression mining indicates that *GAUT3*, *GAUT10* and *GAUT11* are all enriched in root stem cell populations. Through bimolecular fluorescence complementation (BiFC) assays, it appears that GAUT10 can interact with GAUT3 and GAUT11 in the Golgi apparatus. To test the overlapping function of these GAUT proteins during root development, mutant combinations of these four *GAUT* genes have been made. Phenotypic analysis of combinatorial *gaut* seedlings indicate that *GAUT3, GAUT10,* and *GAUT11* have non-redundant and epistatic interactions. Specifically, *gaut11-3* roots are longer compared to wild-type (WT) and loss of *gaut3* and *gaut11* can suppress the short root phenotype of *gaut10*. These results provide new insight into the shared and unique roles of evolutionarily conserved *GAUT* family members during Arabidopsis vegetative development.

CHAPTER 1. INTRODUCTION

Thesis Overview

This thesis is divided into five chapters, general introduction (Chapter 1), the results of my research into the GAUT proteins (Chapter 2), conclusion and next steps (Chapter 3), plant phenotyping via machine learning (Chapter 4), and what is and the development of a data card for an image dataset (Chapter 5). Chapter 1 will be a literature review into the plant cell wall, GAUT proteins, auxin, and Arabidopsis development. Chapter 2 will delve into the results for how several GAUT genes affect Arabidopsis vegetative development. Finally, Chapter 3 will involve the conclusion I have gained from my project as well as the next steps for this project. Chapter 4 will discuss plant phenotyping via machine learning using an Arabidopsis dataset I am developing now. The last chapter, Chapter 5, will go over what is a data card, what entails writing one, and why they are important for datasets.

Literature Review

The Plant Cell Wall

The plant cell wall is vital for external protection, cell-to-cell communication (Jamet and Dunand, 2020), determines cell shape and expansion (Du et al., 2022), and root growth and development (Somssich et al., 2016; Jobert et al., 2023). The cell wall is mainly composed of three polysaccharide classes, which are cellulose, hemicellulose, and pectin (Jobert et al., 2023). Cellulose, hemicellulose, and pectin are all synthesized within the Golgi apparatus (Somssich et al., 2016). Cellulose is a polysaccharide composed of a linear chain of β1,4-linked D-glucose that are synthesized by cellulose synthase complexes (CSCs) in the plasma membrane of land plants (Cosgrove, 2022 and reviewed by Allen et al., 2022). Cellulose is the largest polysaccharide within the plant cell wall (Majda and Robert, 2018).

CMFs have the tendency to form laterally, which in the primary cell walls look like a 2D network of bundled microfibrils (Cosgrove, 2022). Hemicellulose is comprised of a diverse assortment of polymers such as xyloglucans (XyG), mannans, mixed-linked glucans (MLGs), and xylans (Delmer et al., 2024). Even with this diverse group of hemicellulose, most of the hemicellulose mentioned above have a backbone of β-1,4-linked sugars, while MLGs backbones are comprised of β-1,3-linked sugars; however, the listed forms of hemicellulose do have one thing in common, they bind to cellulose (Delmer et al., 2024). In most land plants, xyloglucans comprise the majority of hemicellulose within the primary cell wall (Cosgrove, 2022).

The structure of the plant cell wall is vital for the cells ability to grow/expands and adapt to its surroundings. There have been several models of the plant cell wall and how the components interact. Such as the tethered network model where cellulose microfibrils are tethered by xyloglucan, while another involved looking at the cell wall as a pectic hydrogel that is reinforced by the cellulose microfibrils (reviewed in Cosgrove, 2024). As stated by Cosgrove, 2024; based on years of research a scenario for wall synthesis and assembly could be put together. CSCs are delivered by Golgi vesicles and delivered to the plasma membrane where these CSCs synthesize cellulose microfibrils, xyloglucans will spontaneously bind to cellulose (this reduces cellulose-cellulose contacts); pectin’s bind to the cellulose microfibrils (reviewed in Cosgrove, 2024).

As stated earlier, the plant cell wall is involved in external protection of the cell, but not just in a passive sense. Arabidopsis cell wall mutant, *irregular xylem (irx) 5/3/1*, are defective in CESA subunits that are required secondary cell wall formation showed an increased pathogen resistance (reviewed in Bacete et al., 2018). While pectin has been shown to be involved in penetration resistance and hyphal growth of *Colletotrichum higginsianum* (Engelsdorf et al., 2018). Hemicellulose content and degree of acetylation have been shown to determine disease resistance in plants. It has been shown in several studies that in Arabidopsis *de-etiolateed3* (*det3*) and *irx6* mutants; as well as *xyl1-2* (lead to modification of xyloglucan structure) have an increased resistance to the *P. cucumerina* fungus (reviewed in Bacete et al., 2018). Fragments of the cell wall act as danger-associated molecular patterns (DAMPS), when perceived by the cell they serve as signals for pathogens and/or cell wall integrity issues (reviewed in Wolf, 2022).

This evidence of cell wall pathogen defense was shown in a study testing how the cell wall composition affects pathogen/disease resistance by using 30 Arabidopsis cell wall mutants (*cwm)* and three different pathogens: necrotrophic fungus (*Pc*), vascular bacterium (*Rp*), and biotrophic oomycete (*Hpa*). It was shown that within these 34 *cwm* lines, 29 showed a modified pathogen resistance (mostly enhanced resistance), while within those 29, 18 of the mutants was found to have altered cell wall composition when compared to wild type (Molina et al., 2021). The mutants *at1g23170-1, at1g70770-1, xcp2-1 ago4-1t* had reduced cellulose while *acs8-2* had increased levels of cellulose; *det3-1* and *irx1-6* had decreased pectic uronic acid, with *arr6-3* having increased levels of noncrystalline neutral sugars and *at1g70770* and *acs8-2* having decreased levels (Molina et al., 2021).

Pectin

Pectin is the most abundant form of polysaccharide in the plant cell wall, with pectin making up approximately 30% of the cell wall (Cosgrove, 2022). Pectin is composed of four different classes, homogalacturonan (HG), rhamnogalacturonan I (RG-I) and rhamnogalacturonan II (RG-II), and xylogalacturonans (Jobert et al., 2023). The most abundant form of pectin out of the four pectin classes is homogalacturonan, which accounts of 35% of the primary cell wall in eudicots and nongraminaceous monocots (Atmodjo et al., 2011). RG-I is comprised of repeated GalA and α-1-2-L-rhamnose (Jobert et al., 2023), while RG-2 are shorter polysaccharides comprised of a GalA backbone with four chains that have ten or more different sugars (Jobert et al., 2023). Finally, there are xylogalacturonans (XG) which are less common and are comprised of β-1,4 glucan backbone that have GalA chains and D-xylose residues (Jobert et al., 2023). A family of enzymes called GALACTURONOSYLTRANSFERASES (GAUTs), contribute to pectin composition in Arabidopsis (Caffall et al., 2009 and Atmodjo et al., 2011). Once HG is synthesized there are several enzymes that can/will modifying said HG. Those included PMEs (which de-methylesterify HG), PME inhibitors, acetyl esterase's, and polygalacturonases (hydrolyzes the methyl/acetyl esters and the HG backbone) (reviewed in Delmer et al., 2024).

Pectin is vital for cell wall structure and expansion. Modification in the amount and/or structure of pectin can affect numerous plant phenotypes, including root length seed coat formation, seed dispersal, leaf expansion, and stomatal pore development (Caffall et al., 2009; Du et al., 2022; Guo et al., 2021; Pu et al., 2019; Dash et al., 2023). Pectin methyl-esterification status potentially has the ability to affect phyllotactic patterning in the Arabidopsis shoot apical meristem. Phyllotaxis is the patterning of plant leaves and flowers that has been shown to be controlled by auxin gradients (Peaucelle et al., 2011).

HG is esterified by pectin methyltransferases (PMTs) (Du et al., 2022) and is mainly methyl-esterified (70-80%) when it is deposited within the cell wall and pectin methyl-esterase's (PME) are the ones to de-methyl-esterify HG (Peaucelle et al., 2008). A study from 2008 has provided evidence that when PME is repressed and HG is de-methyl-esterified, the flower primordia is affected. In alcohol inducible *PMEI3* (PMEI's inhibit PME's) lines (PMEI.H1 and H2) had higher PMEI expression resulting in PME repressions, the two lines when in the presence of alcohol have suppressed lateral organ formation in the inflorescence meristem and those with initiated floral meristems before the alcohol treatment developed into deformed flowers that lacked lateral organs (Peaucelle et al., 2008). It was shown that when the alcohol treatment was stopped, the meristem remained functional (was able to produce lateral organs without the presence of alcohol), however, the primordia produced has abnormal phyllotaxis that is abnormally enlarged (Peaucelle et al., 2008).

PMEI13 is not the only protein that has been shown to repress/reduced PMEs, leading to increased dimethyl-esterification and affecting phyllotaxis. BELLRINGER (BLR) is a homeodomain transcription factor that is known for its establishment and maintenance of phyllotaxis in Arabidopsis. A mutant allele of *BLR* gene (*blr-6*) produces ectopic flowers at the shoot apex and differences in primordia angles, the angles between primordia were measured and showed that the *blr-6* mutant had significantly different angle distribution when compared to WT plants (Peaucelle et al., 2011).

To determine if the *blr-6* mutant phyllotaxis defects are the result of cell wall composition change within the shoot apical meristem (SAM). This was achieved by the use of Fourier transform infrared (FTIR) microspectroscopy and the monoclonal antibody 2F4. The FTIR showed that waves that correspond to ester bonds had significantly different absorbance levels between WT and *blr*-6 plants with the *blr*-6 plants have lower HG esterification (Peaucelle et al, 2011). To confirm the FTIR results, the monoclonal antibody 2F4, which labels demethylesterified HG, showed that the *blr-6* mutant had increased and spread-out signal in the primordia when compared to WT plants (Peaucelle et al., 2011). This study presented evidence that this BLR mutant (*blr-6*) does have an effect on phyllotaxis as well as indicating that *blr-6* mutants have increased dimethyl-esterification of pectin within the shoot apical meristem (SAM), leading to changes in the phyllotaxis pattern in Arabidopsis.

As previously mentioned, pectin is synthesized by the GAUT family of proteins. Several studies in Arabidopsis have shown that GAUT1, GAUT4, GAUT10, GAUT11, GAUT13, and GAUT14 are involved in catalytic HG biosynthesis (Engle et al., 2022). GAUT1:GAUT7 have been shown to form a complex in vitro (HEK293 cells) that synthesizes high molecular weight HG in a two-phase model (Amos et al., 2018). In addition, GAUT 5, GAUT6, and GAUT7 have been shown to anchor GAUT1 to the Golgi apparatus within the pollen tube of Arabidopsis, being required for proper pollen germination and elongation (Lund et al., 2020).

GAUT12 is not as studied as the other GAUTs mentioned but it has been implicated in *Populus* and its biomass. In GAUT12 knockdown mutant (*GAUT12.1*) in *Populus trichocarpa*, exhibited 25 to 47% reduction in galacturonic acid as well as 17 to 30% in xylose indicating GAUT12s role in HG and Xylan formation (Biswal et al., 2015). While overexpression lines of *GAUT12.*in *Populus* showed opposite effects. With overexpression lines having increased GalA (12 to 17%) and xylose (14 to 20%) when compared to WT (Biswal et al., 2018). These results from the overexpression study add more evidence to the role of GAUT12 in Xylan and HG formation. GAUT9 has been shown to bind to ELMO, in ELMO mutants the levels of pectin, esterification, and adhesion were reduced potentially indicating ELMO affecting GAUT9s pectin biosynthesis process (Kohorn et al., 2023).Mutants of GAUT8 (QUA1), *qua1-1*, has been shown to have reduced Uronic acid because of lower GalA content (Bouton et al., 2002). However, there is still much unknown on the synthesis and properties of pectin during plant development.

Auxin and the acid growth hypothesis

Auxin is a vital plant hormone responsible for plant growth and development and managing a variety of abiotic and biotic stresses such as drought and temperature (Del Bianco et al., 2023). Indole-3-acetic acid (IAA) is the predominant auxin in most plant tissues. IAA is synthesized from tryptophan via IPyA by TAA enzymes. The IPyA pathways consists of two main steps; the first is the deamination of Trp into IPyA by TRYPTOPHAN AMINOTRANSFERASE OF ARABIDOPSIS 1 (TAA1) and TAA1-RELATED proteins (TARs), second step involves the decarboxylation of IPyA to IAA which is catalyzed by the YUCCA (YUC) family (Casanova-Saez et al., 2021). [describe pathway and cite Casanova-Saez et al., 2021]. While other auxin biosynthesis pathways have been proposed over the years, the IPyA pathway is accepted in the field as the primary mechanism for auxin production in plant tissues.

Auxin has been implicated in regulating both cell division and cell elongation to influence organ growth among other aspects of plant development. Research from 2022 indicates that auxin plays an important role in facilitating the revitalization of cell-wall inorganic phosphorus in phosphorus deficient rice (Huang et al., 2022). The same researchers showed that auxin accelerates the displacement of Pi from the root to shoot, by the interaction between naphaleneacetic acid (NAA) and the Pi transporter gene *OsPT2.* Where there was increased transcript level of *OsPT2* when deprived of Pi and the addition of NAA (Huang et al., 2022). Auxin has been shown to be vital for maintaining a functional root meristem in Arabidopsis from the grafting of WT shoots to *wei8 tar2* roots that showed WT shoot auxin could not compensate for the loss of auxin in the *wei8 tar2* roots (Brumos et al., 2018).

As well as being responsible for the radial initiation of lateral organs. When tomato shoot apices were treated with the auxin transporter inhibitor N-1-naphthylphthalamic acid (NPA), these apices showed inhibited new leaf primordia formation while the meristem continued to grow (Reinhardt et al., 2000). In Arabidopsis *pin1-1* mutants, which have affected auxin transport in the inflorescence stem, these mutants were treated with IAA in lanolin paste, the treatment resulted in the formation of flower primordia (Reinhardt et al., 2000). All this together showed that auxin is vital for proper organ initiation and formation in tomato and Arabidopsis.

The role of auxin in cellular expansion has been described through the acid growth theory (Arsuffi and Braybrook, 2018; Majda and Robert, 2018). In the 1970s, auxin treatment was shown to trigger proton pumps in the plasma membrane, leading to excess H+ in the apoplast and decreased pH, leading to the activation of wall loosening proteins and upregulation of genes related to the cell wall (Rayle and Cleland, 1970 and Hager et al., 1971). Recently, two mechanisms on how auxin effects the cell wall through the acid growth theory have been proposed (reviewed in Jobert et al., 2023).

The first one involves the use of TIR1/AFB receptor proteins, leading to TIR/AFB interacting with AUX/IAA and the eventual expression of ARFs (Reviewed in Salehin et al., 2015, Chapman and Estelle, 2009; Cancé et al., 2022). Within Arabidopsis, there are 6 TIR1/AFBs, 23 auxin response factors (ARFs), and 29 Aux/IAA proteins (Salehin et al., 2015). It has been shown that the Aux/IAAs bind to ARFs which then recruit TOPLESS (TPL), which is a corepressor protein to bind to chromatin (reviewed in Salehin et al., 2015).

While the other mechanism involves extracellular auxin being perceived by AUXIN BINDING PROTEIN 1 (ABP1) and TRANSMEMBRANE DOMAIN KINASE (TMK) (Friml et al., 2022; Yu et al., 2023. ABP1 in Arabidopsis binds to auxin at an acidic pH as seen in the apoplast, this same study provided evidence indicating that APB1 and TMK1 induce an auxin phosphorylation response (Friml et al, 2021). These models do potentially explain the start of acid growth but not what causes the acid-induced wall creep, which has been shown to involved proteins called expansions (EXPAs) (Cosgrove, 2024). These two models may not be mutually exclusive.

The GAUTs

In Arabidopsis, there are 15 GAUT family members and 10 GAUT-like family members (Caffall et al., 2009). The first identified GAUT, GAUT1, has been the most widely studied member of this family. GAUT1 can form a protein complex with GAUT7 comprising the catalytic core of a HG:GalAT complex (Atmodjo et al 2011). GAUT5, GAUT6, and GAUT7 are vital for the production of HG in pollen tubes and can affect the male fertility in Arabidopsis (Lund et al., 2020). While GAUT1, 4, 10, 11, 13, and 14 have been shown to be involved in catalytic HG biosynthesis (Engle et al., 2022). GAUT 13 and GAUT14 are expressed in the male pollen tube were shown to be involved in male fertility in Arabidopsis. In *gaut13 gaut14* double mutants, a reciprocal cross showed that when pollen of the double mutants was used to pollinate WT plants there were no gaut13-1/+; gaut14/+ and gaut13-2/+; gaut14/+ progeny (Wang et al., 2013). However, when wild type pollen was used to pollinate the double mutants, there were gaut13-1/+; gaut14/+ and gaut13-2/+; gaut14/+ progeny (Wang et al., 2013). These crosses showed that double *gaut13, gaut 14* double mutants had affected male fertility but female fertility was untouched. GAUTs have also been shown to be involved in pectin within other plant species besides Arabidopsis.

The GAUT family is conserved in tomato, which includes 15 orthologs and two copies of *GAUT12* (De Godoy et al., 2013). In tomato, GAUT4 is involved in pectin biosynthesis by genetic analyses. It was shown in *GAUT4* silenced plants that leaf cell wall composition was practically unaltered while in the fruits of these plants contained less ammonium oxalate pectin as well as lowered amounts of Rha, Ara, and galactose (De Godoy et al., 2013). Within other plant species, switchgrass (*Panicum virgatum*) and rice (*Oryza sativa*), downregulated *GAUT4* has effects on pectin biosynthesis and sugar release. It was shown in downregulated *GAUT4* (*GAUT4-KD*) that GalA, the main sugar component of HG, was significantly reduced in switchgrass (74-91%0, in rice (69-78%) and in poplar (48-57%) when compared to control plants (Biswal et al., 2018).

GAUT10 is an auxin regulated protein that has a short root phenotype in the absence of sucrose (Pu et al., 2019 and Dash et al., 2023). This protein was found in an auxin root proteomics study, where five-day-old Arabidopsis seedlings were treated with 1 μm of IAA or mock solution for 30 minutes or two hours, then the roots were collected and the proteins were analyzed by mass spectrometry (Pu et al., 2019). During this study it was shown that GAUT10 is downregulated after 120 minutes of auxin treatment and that when *gaut10-3* seedlings were treated with exogenous IAA and grown with sucrose, the *gaut10* seedlings responded normally to auxin (Pu et al., 2019). GAUT10 is required for pectin biosynthesis in Arabidopsis (Caffall et al., 2009 and Engle et al., 2022).There are three *gaut10* T-DNA insertions: *gaut10-1* (knock out), *gaut10-2* (knock down), and *gaut10-3* (null mutant), that each had decreased GalA (Caffall et al., 2009, Pu et al., 2019, and Dash et al., 2023). The short root phenotype of *gaut10* seedlings is due to a reduction in both cell number and cell elongation (Dash et al., 2023).

The sucrose-dependent nature of the *gaut10* phenotype is apparently linked to peroxisome function, indicating potential links between redox status and cell walls (Dash et al., 2023). GAUT10 has also been reported to play a role in stomatal function in concert with GAUT11 (Guo et al., 2021). Specifically, *gaut10 gaut11* double mutants had larger stomata with smaller pore area, which affected stomatal dynamics and drought tolerance (Guo et al., 2021). Many other GAUT family members have been linked to compositional phenotypes, secondary cell wall formation, pollen tube growth, and mucilage formation in seeds (Caffall et al., 2009; Lund et al., 2020; Wang et al., 2013). GAUT proteins can form complexes and may work in concert with one another (Atmodjo et al., 2011 and Lund et al., 2020).

However, how GAUT10 and its co-expressed paralogs (GAUT3, 8, and 11) affect cell wall morphology and composition is still unclear. The research I have conducted, has given a glimpse into the possible roles of GAUT10 and its paralogs in Arabidopsis development. The next chapter will delve into what I have done in terms of GAUT3, 10, and 11, discussing the results that I have achieved and the insight into how these GAUTs affect Arabidopsis.

CHAPTER 2. ROLE OF GAUTS IN ARABIDOPSIS VEGETATIVE DEVELOPMENT

Overview

Loss of function alleles for the GAUT family members of interest have been previously characterized (Caffall et al., 2009; Lewis et al., 2013; Pu et al., 2019; Guo et al., 2022; Dash et al., 2023). In addition to GAUT10, both GAUT3 and GAUT11 are expressed in several root stem cell populations including epidermis (Epi), columella stem cells (CSC), xylem (Xyl), and the quiescent center (QC) (**Fig. 1A**). However, higher order mutant combinations between these three GAUT family members with overlapping expression patterns in the root apical meristem (RAM) have not yet been evaluated. A combinatorial genetic analysis of *gaut3, gaut10,* and *gaut11* will require seven possible mutant combinations (**Table 1**). To date, all but one (*gaut3-1gaut10-3)* of these mutant combinations have been generated and phenotyped (**Fig. 2**) for several morphological characteristics such as primary root length, lateral root density, and hypocotyl length.

Primary Root Length

While most GAUT genes are expressed ubiquitously (Caffall et al., 2009), gene expression mining indicates that *GAUT3*, *GAUT10* and *GAUT11* are all enriched in root stem cells (Clark et al., 2019) (**Fig. 1A**). Loss of *GAUT10* has been shown to shorten primary root length in Arabidopsis in the absence of sucrose (Pu et al., 2019; Dash et al., 2023). In addition, *gaut10 gaut11* double mutant roots were shown to be short under normal growth conditions (Guo et al., 2021).

The single *gaut* mutants were obtained from SALK lines, except for the *gaut10-3 gaut11-3* mutant which has been previously published and was obtained from the authors (Guo et al., 2021 Plant Phys). *gaut11* was obtained after *gaut3-1* was crossed with *gaut10-3 gaut11-3*, from the segregating F2 population. The single, double, and triple mutants were obtained from crossing single and/or double mutant alleles listed in Table 1. Since Arabidopsis are self-pollinators, individual plants were first emasculated and then subsequently pollinated according to the method in Weigel and Glazebrook (2006). To create the *gaut3 guat10* double mutant and *gaut 3 gaut10 gaut11* triple mutant, *guat3-1* and *gaut3-2* were crossed with the *gaut10-3 gaut11-3* double mutant. To create the *gaut8 guat10* double mutant and *gaut 8 gaut10 gaut11* triple mutant, *guat8-1* was crossed with the *gaut10-3 gaut11-3* double mutant.

To verify that the desired crosses were achieved, genotyping was done on individual F1 plants from each cross. After verifying the correct genotypes, the F1 plants were self-pollinated and F2 seed was collected. To recover the desired double and triple mutants (**Table 1**), F2 populations were grown in the growth chamber and each individual seedling was genotyped using polymerase chain reaction (PCR) for all six alleles. **Table 2** outlines the primers used for each allele, sequence of the primers, and optimal temperatures for each. DNA was extracted from 2-week-old leaves from each individual plants and stored at -20°C prior to analysis. All PCRs were analyzed by gel electrophoresis on a 1% agarose gel. Finally, the gels were annotated to determine the allele composition of each plant. Once the final genotype was assigned for each individual plant, seeds were collected and stored in individual envelopes labeled with genotype and date of seed collection.

To measure the primary root length, Arabidopsis seedlings were grown on 0.5X Linsmaier and Skoog (LS) plates supplemented with 0% or 0.5% sucrose. At five-days after germination, the seedlings were imaged, and the primary root lengths were manually measured using Fiji/ImageJ. To determine statistical significance, a two-way ANOVA was performed in Prism. All genotypes tested exhibited normal root lengths in the presence of 0.5% sucrose, except for *gaut3-1gaut11-3* which had longer primary roots than Col-0 (the wild-type control) and *gaut10-3* which had shorter roots compared to Col-0 (**Fig. 3**). Notably, both *gaut3-1* and *gaut11-3* single mutants had wild-type root lengths in the absence of sucrose, but the *guat3-1 gaut11-3* double mutant had longer roots (**Fig. 3**). In addition, the *gaut3-1 gaut10-3 gaut11-3* seedlings also had longer roots than Col-0 when grown on the 0% sucrose plates (**Fig. 3**). This was a surprising result as these genes were predicted to have overlapping functions as other GAUTs have been shown in previous research. These results suggest that GAUT3 and GAUT11 may have overlapping roles in root growth and development which are epistatic to GAUT10.

Lateral Root Density

Lateral root density (LRD) was also examined in various *gaut* combinations as GAUT10 has been previously linked to lateral root formation (Pu et al., 2019). Lateral root density was measured on 9-day-old seedlings grown with and without sucrose by taking the average primary root length (within the specific genotype) and dividing it by number of lateral roots. Differences in LRD was seen in both 0.5% and 0% sucrose treatments. A two-way ANOVA was run on the LRD to determine significance (**Fig. 4)**. There were several differences in LRD within genotype and the two treatments. The genotypes grown with 0.5% sucrose (normal conditions) showed differences in LRD when compared to each other. Specifically, the *gaut3-1 gaut11-3* double mutant had increased LRD when compared to *gaut11-3*. The same can also be said of *gaut3-1 gaut11-3* and *gaut10-3*, with *gaut3-1 gaut11-3* having a higher LRD than *gaut10-3*. This is quite interesting since 0.5X LS plates supplemented with 0.5% sucrose are ‘normal’ conditions and these same genotypes showed WT primary root length under these same conditions, but LRD did not follow this pattern.

The genotypes grown without sucrose showed significant differences in LRD as well. The *gaut3-1gaut11-3* double exhibited increased LRD when compared to Col-0, *gaut3-1* and *gaut11-3. gaut10-3* also had significantly lower LRD when compared to Col-0, which is consistent with our previously reported result (**Fig. 5**). Altogether this preliminary phenotyping indicates that these *GAUT3, GAUT10* and *GAUT11* have additive interactions for lateral root formation.

Preliminary Data into Hypocotyl Length and Stomata Phenotypes

Previous research from Guo et al., 2021 has shown that the loss of *GAUT10* and *GAUT11* can lead to altered stomatal phenotypes and impaired hypocotyl length. Specifically, rosette leaves of *gaut10 gaut11* plants exhibit stomata with a smaller pore area (Guo et al., 2021). The same study reported that *gaut10gaut11* hypocotyls are shorter compared to wild-type controls. Thus, these two GAUT genes may play multiple roles in plant growth in development across many different organs, namely roots, shoots, and leaves.

Hypocotyl length data was obtained from five-day-old seedlings grown in light (**Fig. 6**) conditions on plates supplemented with or without 0.5% sucrose for all genotypes listed in Table 1. Hypocotyl lengths were measured using Fiji/ImageJ software (n=15-20) for each genotype. Statistical analysis was performed using a two-way ANOVA. As seen in Figure 5, there is no discernible difference in hypocotyl length between wild-type and all the *gaut* genotypes tested except for the *gaut3-1 gaut11-3* double mutant. In the absence of sucrose, *gaut3-1 gaut11-3* double mutants exhibited long hypocotyls compared to wild-type Col-0 (**Fig. 7**). Previously, *gaut10 gaut11* double mutants were shown to exhibit short hypocotyls (Guo et al., 2021), but this phenotype was not observed under the growth conditions tested here. This may indicate that these hypocotyl phenotypes are light dependent. Since only light conditions were analyzed, this experiment will need to be repeated with light and dark to determine if this is the case.

Stomata density and shape were examined for qualitative analysis across all genotypes listed in Table 1 (**Fig. 8**). Based on these preliminary images, there three genotypes may exhibit altered stomata density and/or shape compared to Col-0. *gaut3-1* seems to have fewer and smaller stomata compared to Col-0. The stomata of *gaut10 gaut11* double mutants seemed to align with what the previous study found (Guo et at., 2021). The triple mutant *gaut3-1 gaut10-3 gaut11-3* stomata appear to have thinner guard cells. These results would need to be further replicated and quantified to determine statistical significance.

CHAPTER 3. CONCLUSION AND NEXT STEPS

Conclusion

There is still much to be done with GAUT10 and its paralogs in how they affect Arabidopsis development. So far, I have shown that GAUT3, GAUT10, and GAUT 11, contribute to primary root length, LRD, hypocotyl length, and stomata development. These three GAUT genes display additive effects in LRD but more complex genetic interactions in other traits. Whereas *gaut10-3* and *gaut10-3 gaut11-3* have short root phenotypes, *gaut3-1 gaut11-3* and *gaut3-1 gaut10-3 gaut11-3* have long primary root phenotypes. This suggests that *GAUT10* and *GAUT11* are functionally overlapping but epistatic to *GAUT3*. During lateral root development, a complex genotype x treatment effect was observed among the various *gaut* alleles examined. In the presence of sucrose, *gaut3-1 gaut11-3* and *gaut3-1 gaut10-3 gaut11-3* exhibited higher LRD compared to wild-type and single mutant controls. In contrast, in the absence of sucrose the *gaut3-1 gaut10-3 gaut11-3* has normal LRD. These data suggest that sucrose may influence lateral root formation when cell wall composition is altered.

The contributions of GAUT3, GAUT10, and GAUT11 to hypocotyl growth appears to be complex. Under light grown conditions without sucrose, *gaut3-1 gaut11-3* seedlings had longer hypocotyls. Previously, it was reported that *gaut10-3 gaut11-3* hypocotyls were short (Guo et al., 2021). The loss of all three *GAUT* genes in the triple mutant (*gaut3-1 gaut10-3 gaut11-3*) appeared to restore hypocotyls to wild-type length. Given that hypocotyl length is driven solely by cell elongation, whereas primary root growth and LRD are a product of cell division and elongation, these results suggest that cell wall composition may have different impacts on growth properties within an organ.

Next Steps

Determining the roles of GAUT10 and its paralogs in Arabidopsis growth and development

Further examination of hypocotyl lengths

The hypocotyl length for *guat10* and other desired *gaut* mutant combinations (**Table 1**) will be measured in light and dark grown seedlings using Fiji/ImageJ. 15-20 seedlings of each genotype will be grown to five-days-old on 0.5X LS supplemented with 0% or 0.5% sucrose, under light and dark grown conditions. Both light and dark grown hypocotyl lengths will be measured since *GAUT3, GAUT10*, and *GAUT11* are expressed within the hypocotyl and the hypocotyl grows exclusively through cell elongation. These assays will be performed at least three times with the conditions mentioned above. A two-way ANOVA will then be performed on the hypocotyl lengths to determine if there is a significant different between genotype and/or treatment (with/without sucrose). It is expected that *guat10-3 gaut11-3* seedlings will have shorter hypocotyls compared to Col-0 because that has been previously published (Guo et al., 2021).

Quantification of stomata phenotypes

Previous research has shown *gaut10-3 gaut11-3* stomata had a larger stomatal complex with a smaller pore area (Guo et al., 2021). Also, through my own preliminary data, *gaut3-1* potentially has lower stomata density. The stomata shape and density in *gaut* rosette leaves will be examined (Table 1) using scanning electron microscopy (SEM) to determine if there is any difference in stomata shape and density. Six plants from each genotype (**Table 1**) with 1-2 leaves taken from each plant. The stomata on the abaxial surface of 3-week-old leaves will be imaged using the benchtop SEM, and the density, pore area, pore length, and guard cell (GC) pair height, and GC width will be measured with Fiji/ImageJ (Guo et al., 2021). Statistical significance will be evaluated using two-way ANOVA with a p-value of 0.5.

Seed mucilage phenotyping

Seed mucilage is composed of pectin and hemicellulose with the exact polysaccharide makeup being dependent on the species (Tsai et al., 2021). It has been shown that seed mucilage influences several processes like seed germination, seedling establishment, and potentially maintaining water during drought conditions (Tsai et al., 2021). Previous research has shown *gaut10* and *gaut11* seeds have reduced mucilage compared to wild type (Caffall et al., 2009; Guo et al., 2021). To determine if GAUT10 and the other co-expressed GAUT members also contribute to seed mucilage production in Arabidopsis, ruthenium red staining will be performed as previously described (Guo et al., 2021 and McFarlane et al., 2014). For each genotype, ~20 of seeds will be stained and imaged on a dissecting microscope.

Characterizing the influence of auxin on cell wall composition during Arabidopsis root development

Characterizing the composition of the cell wall in collaboration with the Dr. Olga Zabotina as we previously have done (Dash et al., 2023). Research from 2023 has shown that in *gaut10-3* roots grown under 0.5% sucrose did have reduced GalA levels in the pectin enriched fraction of a monosaccharide composition analysis (Dash et al., 2023). As well as 15 differentially enriched polysaccharide epitopes and 12 hemicellulose epitopes. Specifically, a subset of the genotypes listed in Table 1 will be grown to five-days-old on 0.5% sucrose. These experiments will provide insight into whether the paralogs of GAUT10 will affect the compositions of the cell wall and to investigate if/how cell wall composition could influence auxin pathways, such as what has been shown in previous research (Dash et al., 2023). Then in collaboration with the Zabotina lab, we will perform epitope and full glycome profiling to determine if there is any significant difference. This will be done with Enzyme-linked immunosorbent assay (ELISA). ELISA is a biomedical technique that uses antibodies to detect the presence of antigens such as proteins, hormones, and monosaccharides, etc. (Gan and Patel, 2013). As done in Dash et al., 2023, select genotypes as listed in Table 1, will be processed for epitope and/or full glycome profiling. There will be 3 biological replicates and the use of 2-sample nonparametric Wilcoxon rank-sum test and the use of Enzyme-linked immunosorbent assay (ELISA) for the full glycome profiling (Dash et al., 2023). With this profiling of the genotypes, hopefully, provide insight into whether the *gaut* mutants will have differences in their monosaccharide composition and/or epitope profiles.

CHAPTER 4. PLANT PHENOTYPING VIA MACHINE LEARNING

Introduction into machine learning

The increase of machine learning (ML) and artificial intelligence (AI) offers a wide variety of tools that could be used in the analysis of biological data. Machine learning can be defined as fitting predictive models to data in an attempt to mimic human thinking (Greener et al., 2022). ML and AI has the ability to measure the phenotypes of biological samples such as cell number and primary root length within plants as well as create realistic images. However, when it comes to biological data and machine learning there are several challenges that hinder progress. First, one of these issues is data availability; some areas of biology contain a multitude of data (Greener et al., 2022) while other areas are lacking data. ML can be categorized into two types of ML: supervised learning and unsupervised learning.

Supervised learning is where instances (standardized form of set objects) have the correct objects label which is the training data set; a model then uses this training set to train and then predict labels for new instances for which the correct label is not known (Kan, 2017). Unsupervised learning is where there is no category or features that is the label, this method of ML is used to explore data structure (Kan, 2017). There are a multitude of models to fit the type of data you wish to analyze such as using 2D CNNs and residual networks to analyze image datasets while 1D CNNs work best for gene sequences (Greener et al., 2022).

Even with these ML and AI tools available, many tasks such as image analysis for Arabidopsis are just emerging in the ML image analysis space. For example, a paper in 2021 described a ML based approach for high-throughput hypocotyl phenotyping (Dobos et al. 2019), a robotic based assay combined with ML has also been used to phenotype rosette leaves (Xiang et al., 2021), In addition, one study focused on root phenotyping has also leveraged ML (Yasrab et al., 2019). However, there has not yet been a ML based method for simultaneously phenotyping the numerous organs and morphological traits of Arabidopsis seedlings: root length and branching, hypocotyl length and width, and cotyledon size. Such a tool would be valuable to the community to provide an integrated approach to seedling trait phenotyping, rather than focusing on individual organs.

Machine learning in plant phenotyping

A recent technique for root phenotyping image analyzing is RhizoVision Explorer paired with RootPainter which is a deep learning segmentation for biological images (Smith et al., 2022). RhizoVision is an open-source software that provides reliable and fast image processing of plant roots (Seethepalli et al., 2021). RhizoVision has the ability to extract a number of root feature such as number of root tips, number of branch points, root length, etc., which would greatly increase researchers' ability to phenotype a vast number of root samples and root phenotypes. RhizoVision was compared to several other root image software in many root features to determine which program provided more accurate results.

It was shown that RhizoVision slightly overestimated root length while IJ_Rhizo overestimated length and WinRhizo slightly underestimated root length (Seethepalli et al., 2021), RhizoVision was slightly more accurate than the other two programs. While in surface area and average diameter, all three software's were close together in accuracy. Volume was another feature that RhizoVision excelled in, with it having a strong agreement between the estimated volume and the ground truth volume. While IJ_Rhizo and WinRhizo had a lower agreement between estimated volume and ground truth volume (Seethepalli et al., 2021) However, RhizoVison has only been trained on herbaceous species such as Maize and wheat, which are plants that have much larger root systems that Arabidopsis.

RootPainter is an open-source graphical user interface software that can be used to train deep neural networks such as Convolutional neural networks (CNNs) to analyze biological images such as plant roots (Smith et al., 2022). CNNs are a type of deep-learning model that is comprised of three main layers: the convolutional layers, pooling layers, and the fully connected layers; convolutional layers that involve the use of kernels to convolve the image into feature maps, pooling layers reduce the width and height of the input for the next layers, and the fully connected layers contain the neural network (Voulodimos et al., 2018). RootPainter was able to train a deep-learning model on three different datasets with different targets and image qualities (including background and image quality) with high accuracy and a relatively short (< 2 hour) computing time (Smith et al., 2022).

As stated earlier, ML methods for Arabidopsis are just recently emerging in the field of image analysis via machine learning. A recent ML method involved the use of deep learning to phenotyping the hypocotyl of Arabidopsis. This deep learning method involved the use of U-Net deep CNN for segmentation, in this case segmenting the image in three parts: background, hypocotyl, and non-hypocotyl (Dobos et al., 2019). This deep learning method was test on ~2,500 hypocotyls with several different conditions such as light/no light and differing light wavelengths. It was shown that the algorithm performed on par with the two human experts, with higher accuracy, precision, and recall with the Arabidopsis and Brachypodium hypocotyls, demonstrating its ability to accurately analyze hypocotyls akin to trained human experts (Dobos et al., 2019). A bonus of this method is it ability to phenotypes images that are low-quality such as phone images or those from a flatbread scanner.

Another phenotyping system is using RoAD: Robotic Assay for Drought, which can automatically phenotype brassinosteriod (BR) and drought response (Xiang et al., 2021). RoAD is a fully automated assay that includes a robotic arm, rover, bench scale, a controlled water system, RGB camera, and a laser profilometer; with all this equipment, plants in soil can be automatically watered with BR biosynthesis inhibitor Propiconazole (Xiang et at., 2021). Along with this fully automated system and ML algorithms (a phenotyping pipeline designed by the researchers of this study), was able to accurately phenotype traits such as leaf length and width with high R-squared value (Xiang et al., 2021).

The final method is another deep learning approach but analyzing plant root architectures, called RootNav 2.0. RootNav 2.0 used a CNN that segments the root structure and localizes the key points, three metrics are used to test the accuracy of this approach: mean average pixel classification accuracy (global and class) and mean intersection over union (Yasrab et al., 2019). RootNav.2,0 was tested against five other CNN architectures: VGG, FCN, SegNet, UNet, and DeepLab-V3, with the three metrics mentioned above. It was shown that RootNav.2.0 had higher global, class average accuracy, and mean intersection over union when compared to the other CNN architectures (Yasrab et al., 2019). An advantage of this method is ability to transfer learning to different species and images, the CNN was trained on wheat then retrained using ~277 Arabidopsis images on agar plates (Yasrab et al., 2019).

For 60% of the images, all the plants were analyzed, 6% of images one plant was missed, with 20% of the images counting an extra plant, and 14% of the images overcounting more than one plant; besides this RootNav.2.0 measurements did have high correlation with ground truth measurements in root length (Yasrab et al., 2019). However, a drawback from this method is that the images must be high quality which isn't always possible depending on the lab resources.

Arabidopsis is lacking in programs that can perform multi-feature phenotyping, this greatly reduces researchers' abilities to phenotype a great deal of plant features and large number of plants in a short amount of time. Arabidopsis is a relatively small plant compared to Maize or wheat, with 5-day-old primary root length being on average 1-2 cm's for Col-0 grown on 0.5LS media with 0.5% sucrose. This can make imaging and phenotyping by hand these roots a tedious and long process and could be a potential roadblock for ML programs to measure the phenotypes of Arabidopsis.

CHAPTER 5. ARABIDOPSIS SEEDLING DATASET AND DATA CARD

What is a data card?

A data card is a document that summarize the facts of ML datasets that is used to increase responsible AI development; data cards contain information concerning the dataset that cannot be directly obtained from the dataset itself (Pushkarna et al., 2022). According to the previous source, their data card has been designed in a way to promote transparency, scaling in production contexts, and fluency-agnostic readability by containing five key principles: flexible, modular, extensible, accessible, and content-agnostics. The authors of this paper have designed a comprehensive data card template (The Data Card Playbook) to guide creators in the dataset/data card process.

This is the template that I have decided to use to write the data card of my dataset, 5-day-old Arabidopsis seedlings. The advantage of using such data card templates is the ability to organize all the background information of your dataset in an easily accessible way. Data cards include any noise that may be a part of the images, such as condensation or imperfect background. As well as information on how the ground truth was attained, for example how the length of the roots was obtained and what software was used.

Method for making dataset and data card

This dataset is comprised of five-day-old *Arabidopsis thaliana* that were grown to phenotype primary root length based on genotype and/or sucrose treatment. The seedlings are comprised of eight different genotypes (**Table 1**) that were grown on 0.5X Linsmaier and Skoog (LS) plates with or without 0.5% sucrose (example presented in **Fig.9**). After the seeds were sterilized with a 1% bleach solution and plated (approximately 15-20 seeds per plate), they were checked for germination and at five-days-old were imaged ay 800 resolutions with the label on the plate visible and a standard ruler used for measurement scale. To obtain a substantial number of images for image analysis by way of machine learning, each plate (which contained 15-20 seedlings each) were cropped to showcase one seedling per image. This was done by a semi-automatic way through the use of a MATLAB code designed by Laura Zinnel. The process of using this code involves choosing the directory (where your images are located), then the size of the newly cropped image (w x h), and how many crops you want from the image.

Then an image from the image folder (your chosen directory) will then open on the screen, you then crop you desired section. The program will then crop every image in a similar manner as to how you cropped the first image. The code produces a folder title “original folder name_cropped” where the images will then be deposited. After this you can then modify the parameter in the original cropping script and crop the already cropped images as much as you need too. Since my seedlings were not evenly spaced as desired, the images have slight modifications to them. Using Adobe Photoshop, any individual seedling images that contained any extra seedlings or foreign material were removed as long as they did not overlap with the primary image seedling. None of the physical traits of the images were modified, none of the seedling’s hypocotyls, cotyledons, primary root, etc. were added to or removed; just background noise was removed if possible.

When using this MATLAB code, it is important to review all the cropped images since there can be error. For example, if your seedlings are not evenly spaced an image and have multiple seedlings or if the image width and height are too small, parts of the seedling could be cut off. If possible, having some sort of scale, such as the gridlines on the petri dish, within the image would be ideal, so you would need to find the right height and width to achieve this. This process would still require a review of cropped images produced from this program to ensure they are ideal ML images. This process was then repeated on all replicates I have done, three replicates, and the images where polished and renamed.

Conclusion

The purpose of having a data card it to include information one cannot obtained from just looking at the dataset. It will have the process of obtaining the dataset such as how the seedlings where grown, what was used to obtain the ground truth (in this case using Fiji to measure root length), and what noise could affect the training of a machine learning based model. It could also include information on the balance of the dataset, such as if there are more or less long primary roots (> 1 cm) compared to shorter primary roots (< 1 cm). All of these points within the data card can help guide what ML technique works best for the dataset and/or the types of augmentation (such as removing the background or brightening the image) that may need to be performed to improve the images for a ML model. From the seedlings in my dataset, the hope is that multiple traits could be quantified, these are primary root length, hypocotyl length, and cotyledon shape.

The two main tasks I wish to achieve with this data card and the Arabidopsis seedling dataset it to identify risks and to measure the dependability in the data science lifecycle through the use of a data card and to develop new methods and tools for mitigating risk in the data science. The hope is that with this dataset and the data card, the two tasks above can be achieved as well as the Kelley lab and other researchers being able to train/test ML approaches that could multi-phenotype Arabidopsis seedlings which would greatly increases the amount of information that can be gained. As well as lessen the time and effort it takes to phenotype a large amount of Arabidopsis seedlings. Machine learning techniques can be a great help in the field of biological science, especially in image analysis for the end goal of phenotyping, the data card and dataset I have curated can help improve ML in image analysis.

REFERENCES

Allen, Holly, Donghui Wei, Ying Gu, and Shundai Li. "A Historical Perspective on the Regulation of Cellulose Biosynthesis." *Carbohydrate Polymers* 252 (January 15, 2021): 117022. https://doi.org/10.1016/j.carbpol.2020.117022.

Amos, Robert A., Sivakumar Pattathil, Jeong-Yeh Yang, Melani A. Atmodjo, Breeanna R. Urbanowicz, Kelley W. Moremen, and Debra Mohnen. "A Two-Phase Model for the Non-Processive Biosynthesis of Homogalacturonan Polysaccharides by the GAUT1:GAUT7 Complex." *The Journal of Biological Chemistry* 293, no. 49 (December 7, 2018): 19047–63. https://doi.org/10.1074/jbc.RA118.004463.

Arsuffi, Giulia, and Siobhan A Braybrook. "Acid Growth: An Ongoing Trip." *Journal of Experimental Botany* 69, no. 2 (January 4, 2018): 137–46. https://doi.org/10.1093/jxb/erx390.

Atmodjo, Melani A., Yumiko Sakuragi, Xiang Zhu, Amy J. Burrell, Sushree S. Mohanty, James A. Atwood, Ron Orlando, Henrik V. Scheller, and Debra Mohnen. "Galacturonosyltransferase (GAUT)1 and GAUT7 Are the Core of a Plant Cell Wall Pectin Biosynthetic Homogalacturonan:Galacturonosyltransferase Complex." *Proceedings of the National Academy of Sciences* 108, no. 50 (December 13, 2011): 20225–30. https://doi.org/10.1073/pnas.1112816108.

Bacete, Laura, Hugo Mélida, Eva Miedes, and Antonio Molina. "Plant Cell Wall-Mediated Immunity: Cell Wall Changes Trigger Disease Resistance Responses." *The Plant Journal* 93, no. 4 (2018): 614–36. https://doi.org/10.1111/tpj.13807.

Biswal, Ajaya K., Zhangying Hao, Sivakumar Pattathil, Xiaohan Yang, Kim Winkeler, Cassandra Collins, Sushree S. Mohanty, et al. "Downregulation of GAUT12 in Populus Deltoides by RNA Silencing Results in Reduced Recalcitrance, Increased Growth and Reduced Xylan and Pectin in a Woody Biofuel Feedstock." *Biotechnology for Biofuels* 8 (March 12, 2015): 41. https://doi.org/10.1186/s13068-015-0218-y.

Biswal, Ajaya K., Melani A. Atmodjo, Sivakumar Pattathil, Robert A. Amos, Xiaohan Yang, Kim Winkeler, Cassandra Collins, et al. "Working towards Recalcitrance Mechanisms: Increased Xylan and Homogalacturonan Production by Overexpression of GAlactUronosylTransferase12 (GAUT12) Causes Increased Recalcitrance and Decreased Growth in Populus." *Biotechnology for Biofuels* 11 (January 17, 2018): 9. https://doi.org/10.1186/s13068-017-1002-y.

Biswal, Ajaya K., Melani A. Atmodjo, Mi Li, Holly L. Baxter, Chang Geun Yoo, Yunqiao Pu, Yi-Ching Lee, et al. "Sugar Release and Growth of Biofuel Crops Are Improved by Downregulation of Pectin Biosynthesis." *Nature Biotechnology* 36, no. 3 (March 2018): 249–57. https://doi.org/10.1038/nbt.4067.

Bouton, Sophie, Edouard Leboeuf, Gregory Mouille, Marie-Thérèse Leydecker, Joël Talbotec, Fabienne Granier, Marc Lahaye, Herman Höfte, and Hoai-Nam Truong. "QUASIMODO1 Encodes a Putative Membrane-Bound Glycosyltransferase Required for Normal Pectin Synthesis and Cell Adhesion in Arabidopsis." *The Plant Cell* 14, no. 10 (October 1, 2002): 2577–90. https://doi.org/10.1105/tpc.004259.

Brumos, Javier, Linda M. Robles, Jeonga Yun, Thien C. Vu, Savannah Jackson, Jose M. Alonso, and Anna N. Stepanova. "Local Auxin Biosynthesis Is a Key Regulator of Plant Development." *Developmental Cell* 47, no. 3 (November 5, 2018): 306-318.e5. https://doi.org/10.1016/j.devcel.2018.09.022.

Caffall, Kerry H., Sivakumar Pattathil, Sarah E. Phillips, Michael G. Hahn, and Debra Mohnen. "*Arabidopsis Thaliana* T-DNA Mutants Implicate *GAUT* Genes in the Biosynthesis of Pectin and Xylan in Cell Walls and Seed Testa." *Molecular Plant* 2, no. 5 (September 1, 2009): 1000–1014. https://doi.org/10.1093/mp/ssp062.

Cancé, Coralie, Raquel Martin-Arevalillo, Kenza Boubekeur, and Renaud Dumas. "Auxin Response Factors Are Keys to the Many Auxin Doors." *New Phytologist* 235, no. 2 (2022): 402–19. https://doi.org/10.1111/nph.18159.

Casanova-Sáez, Rubén, Eduardo Mateo-Bonmatí, and Karin Ljung. "Auxin Metabolism in Plants." *Cold Spring Harbor Perspectives in Biology* 13, no. 3 (March 2021): a039867. https://doi.org/10.1101/cshperspect.a039867.

Chapman, Elisabeth J., and Mark Estelle. "Mechanism of Auxin-Regulated Gene Expression in Plants." *Annual Review of Genetics* 43, no. Volume 43, 2009 (December 1, 2009): 265–85. https://doi.org/10.1146/annurev-genet-102108-134148.

Clark, Natalie M., Eli Buckner, Adam P. Fisher, Emily C. Nelson, Thomas T. Nguyen, Abigail R. Simmons, Maria A. de Luis Balaguer, et al. "Stem-Cell-Ubiquitous Genes Spatiotemporally Coordinate Division through Regulation of Stem-Cell-Specific Gene Networks." *Nature Communications* 10, no. 1 (December 6, 2019): 5574. https://doi.org/10.1038/s41467-019-13132-2.

Cosgrove, Daniel J. "Building an Extensible Cell Wall." *Plant Physiology* 189, no. 3 (July 1, 2022): 1246–77. https://doi.org/10.1093/plphys/kiac184.

Cosgrove, Daniel J. "Structure and Growth of Plant Cell Walls." *Nature Reviews Molecular Cell Biology* 25, no. 5 (May 2024): 340–58. https://doi.org/10.1038/s41580-023-00691-y.

Cosgrove, Daniel J. "Plant Cell Wall Loosening by Expansins." *Annual Review of Cell and Developmental Biology*, May 9, 2024. https://doi.org/10.1146/annurev-cellbio-111822-115334.

Dash, Linkan, Sivakumar Swaminathan, Jan Šimura, Caitlin Leigh P Gonzales, Christian Montes, Neel Solanki, Ludvin Mejia, Karin Ljung, Olga A Zabotina, and Dior R Kelley. "Changes in Cell Wall Composition Due to a Pectin Biosynthesis Enzyme GAUT10 Impact Root Growth." *Plant Physiology* 193, no. 4 (December 1, 2023): 2480–97. https://doi.org/10.1093/plphys/kiad465.

Del Bianco, Marta, Jiří Friml, Lucia Strader, and Stefan Kepinski. "Auxin Research: Creating Tools for a Greener Future." *Journal of Experimental Botany* 74, no. 22 (December 1, 2023): 6889–92. https://doi.org/10.1093/jxb/erad420.

Delmer, Deborah, Richard A Dixon, Kenneth Keegstra, and Debra Mohnen. "The Plant Cell Wall—Dynamic, Strong, and Adaptable—Is a Natural Shapeshifter." *The Plant Cell* 36, no. 5 (February 1, 2024): 1257–1311. https://doi.org/10.1093/plcell/koad325.

Di, Dong-Wei., Zhang, Caiguo., Luo, Pan., An, Chen-Wei. and Guo, Guang-Qin. "The biosynthesis of auxin: how many paths truly lead to IAA?" *Plant Growth Regul* **78**, 275–285 (2016). DOI 10.1007/s10725-015-0103-5.

Dobos, Orsolya, Peter Horvath, Ferenc Nagy, Tivadar Danka, and András Viczián. "A Deep Learning-Based Approach for High-Throughput Hypocotyl Phenotyping." *Plant Physiology* 181, no. 4 (October 21, 2019): 1415. https://doi.org/10.1104/pp.19.00728.

Du, Juan, Charles T. Anderson, and Chaowen Xiao. "Dynamics of Pectic Homogalacturonan in Cellular Morphogenesis and Adhesion, Wall Integrity Sensing and Plant Development." *Nature Plants* 8, no. 4 (April 2022): 332–40. https://doi.org/10.1038/s41477-022-01120-2.

Engle, Kristen A., Robert A. Amos, Jeong-Yeh Yang, John Glushka, Melani A. Atmodjo, Li Tan, Chin Huang, Kelley W. Moremen, and Debra Mohnen. "Multiple Arabidopsis Galacturonosyltransferases Synthesize Polymeric Homogalacturonan by Oligosaccharide Acceptor-Dependent or de Novo Synthesis." *The Plant Journal* 109, no. 6 (2022): 1441–56. https://doi.org/10.1111/tpj.15640.

Engelsdorf, Timo, Nora Gigli-Bisceglia, Manikandan Veerabagu, Joseph F. McKenna, Lauri Vaahtera, Frauke Augstein, Dieuwertje Van der Does, Cyril Zipfel, and Thorsten Hamann. "The Plant Cell Wall Integrity Maintenance and Immune Signaling Systems Cooperate to Control Stress Responses in Arabidopsis Thaliana." *Science Signaling* 11, no. 536 (June 26, 2018): eaao3070. https://doi.org/10.1126/scisignal.aao3070.

Friml, Jiří, Michelle Gallei, Zuzana Gelová, Alexander Johnson, Ewa Mazur, Aline Monzer, Lesia Rodriguez, et al. "ABP1–TMK Auxin Perception for Global Phosphorylation and Auxin Canalization." *Nature* 609, no. 7927 (September 2022): 575–81. https://doi.org/10.1038/s41586-022-05187-x.

Gan, Stephanie D., and Kruti R. Patel. "Enzyme Immunoassay and Enzyme-Linked Immunosorbent Assay." *Journal of Investigative Dermatology* 133, no. 9 (September 1, 2013): 1–3. https://doi.org/10.1038/jid.2013.287.

Greener, Joe G., Shaun M. Kandathil, Lewis Moffat, and David T. Jones. "A Guide to Machine Learning for Biologists." *Nature Reviews Molecular Cell Biology* 23, no. 1 (January 2022): 40–55. https://doi.org/10.1038/s41580-021-00407-0.

Godoy, Fabiana de, Luisa Bermúdez, Bruno Silvestre Lira, Amanda Pereira de Souza, Paula Elbl, Diego Demarco, Saleh Alseekh, et al. "Galacturonosyltransferase 4 Silencing Alters Pectin Composition and Carbon Partitioning in Tomato." *Journal of Experimental Botany* 64, no. 8 (May 2013): 2449–66. https://doi.org/10.1093/jxb/ert106.

Guo, Huimin, Chuanlei Xiao, Qing Liu, Ruiying Li, Zhiqiang Yan, Xuan Yao, and Honghong Hu. "Two Galacturonosyltransferases Function in Plant Growth, Stomatal Development, and Dynamics." *Plant Physiology* 187, no. 4 (December 1, 2021): 2820–36. https://doi.org/10.1093/plphys/kiab432.

Hager, Achim, Helga Menzel, and Annelore Krauss. "Versuche und Hypothese zur Primärwirkung des Auxins beim Streckungswachstum." *Planta* 100, no. 1 (March 1, 1971): 47–75. https://doi.org/10.1007/BF00386886.

Huang, Jing., Wu, Qi., Jing, Huai. K., Shen, Ren. F. & Zhu, Xiao. F. "Auxin facilitates cell wall phosphorus reutilization in a nitric oxide-ethylene dependent manner in phosphorus deficient rice (Oryza sativa L.)". *Plant Science* **322,** 111371 (2022). https://doi.org/10.1016/j.plantsci.2022.111371

Jamet, Elisabeth, and Christophe Dunand. "Plant Cell Wall Proteins and Development." *International Journal of Molecular Sciences* 21, no. 8 (January 2020): 2731. https://doi.org/10.3390/ijms21082731.

Jobert, François, Sandeep Yadav, and Stéphanie Robert. "Auxin as an Architect of the Pectin Matrix." *Journal of Experimental Botany* 74, no. 22 (December 1, 2023): 6933–49. https://doi.org/10.1093/jxb/erad174.

Kan, Andrey. "Machine Learning Applications in Cell Image Analysis." *Immunology & Cell Biology* 95, no. 6 (2017): 525–30. https://doi.org/10.1038/icb.2017.16.

Kasahara, Hiroyuki. "Current aspects of auxin biosynthesis in plants. *Bioscience, Biotechnology, and Biochemistry"* **80**, 34–42 (2016). http://dx.doi.org/10.1080/09168451.2015.1086259

Kohorn, Bruce D., Nuoya Yang, Margaret Weinstock, Garrison Asper, Isabel Ball, and Devaki Rajiv. "Golgi ELMO1 Binds QUA1, QUA2, GAUT9, and ELMO4 and Is Required for Pectin Accumulation in Arabidopsis." *PLOS ONE* 18, no. 11 (November 8, 2023): e0293961. https://doi.org/10.1371/journal.pone.0293961.

Lund, Christian Have, Anne Stenbæk, Melani A. Atmodjo, Randi Engelberth Rasmussen, Isabel E. Moller, Simon Matthé Erstad, Ajaya Kumar Biswal, Debra Mohnen, Jozef Mravec, and Yumiko Sakuragi. "Pectin Synthesis and Pollen Tube Growth in Arabidopsis Involves Three GAUT1 Golgi-Anchoring Proteins: GAUT5, GAUT6, and GAUT7." *Frontiers in Plant Science* 11 (September 11, 2020). https://doi.org/10.3389/fpls.2020.585774.

Majda, Mateusz, and Stéphanie Robert. "The Role of Auxin in Cell Wall Expansion." *International Journal of Molecular Sciences* 19, no. 4 (April 2018): 951. https://doi.org/10.3390/ijms19040951.

McFarlane, Heather. E., Gendre, Delphine. and Western, Tamara. L. "Seed Coat Ruthenium Red Staining Assay." *Bio-protocol* 4(7): e1096. (April 5, 2014). DOI: 10.21769/BioProtoc.1096.

Molina, Antonio, Eva Miedes, Laura Bacete, Tinguaro Rodríguez, Hugo Mélida, Nicolas Denancé, Andrea Sánchez-Vallet, et al. "Arabidopsis Cell Wall Composition Determines Disease Resistance Specificity and Fitness." *Proceedings of the National Academy of Sciences* 118, no. 5 (February 2, 2021): e2010243118. https://doi.org/10.1073/pnas.2010243118.

Peaucelle, Alexis, Romain Louvet, Jorunn N. Johansen, Herman Höfte, Patrick Laufs, Jérome Pelloux, and Grégory Mouille. "*Arabidopsis* Phyllotaxis Is Controlled by the Methyl-Esterification Status of Cell-Wall Pectins." *Current Biology* 18, no. 24 (December 23, 2008): 1943–48. https://doi.org/10.1016/j.cub.2008.10.065.

Peaucelle, Alexis, Romain Louvet, Jorunn N. Johansen, Fabien Salsac, Halima Morin, Françoise Fournet, Katia Belcram, et al. "The Transcription Factor BELLRINGER Modulates Phyllotaxis by Regulating the Expression of a Pectin Methylesterase in Arabidopsis." *Development* 138, no. 21 (November 1, 2011): 4733–41. https://doi.org/10.1242/dev.072496.

Pu, Yunting, Justin W. Walley, Zhouxin Shen, Michelle G. Lang, Steven P. Briggs, Mark Estelle, and Dior R. Kelley. "Quantitative Early Auxin Root Proteomics Identifies GAUT10, a Galacturonosyltransferase, as a Novel Regulator of Root Meristem Maintenance *[S]." *Molecular & Cellular Proteomics* 18, no. 6 (June 1, 2019): 1157–70. https://doi.org/10.1074/mcp.RA119.001378.

Pushkarna, Mahima, Andrew Zaldivar, and Oddur Kjartansson. "Data Cards: Purposeful and Transparent Dataset Documentation for Responsible AI." In *2022 ACM Conference on Fairness, Accountability, and Transparency*, 1776–1826. Seoul Republic of Korea: ACM, 2022. https://doi.org/10.1145/3531146.3533231.

Rayle, David L., and Robert Cleland. "Enhancement of Wall Loosening and Elongation by Acid Solutions 1." *Plant Physiology* 46, no. 2 (August 1, 1970): 250–53. https://doi.org/10.1104/pp.46.2.250.

Reinhardt, Didier, Therese Mandel, and Cris Kuhlemeier. "Auxin Regulates the Initiation and Radial Position of Plant Lateral Organs." *The Plant Cell* 12, no. 4 (April 2000): 507–18.

Salehin, Mohammad, Rammyani Bagchi, and Mark Estelle. "SCFTIR1/AFB-Based Auxin Perception: Mechanism and Role in Plant Growth and Development." *The Plant Cell* 27, no. 1 (January 1, 2015): 9–19. https://doi.org/10.1105/tpc.114.133744.

Seethepalli, Anand, Kundan Dhakal, Marcus Griffiths, Haichao Guo, Gregoire T Freschet, and Larry M York. "RhizoVision Explorer: Open-Source Software for Root Image Analysis and Measurement Standardization." *AoB Plants* 13, no. 6 (September 13, 2021): plab056. https://doi.org/10.1093/aobpla/plab056.

Smith, Abraham George, Eusun Han, Jens Petersen, Niels Alvin Faircloth Olsen, Christian Giese, Miriam Athmann, Dorte Bodin Dresbøll, and Kristian Thorup-Kristensen. "RootPainter: Deep Learning Segmentation of Biological Images with Corrective Annotation." *New Phytologist* 236, no. 2 (2022): 774–91. https://doi.org/10.1111/nph.18387.

Somssich, Marc, Ghazanfar Abbas Khan, and Staffan Persson. "Cell Wall Heterogeneity in Root Development of Arabidopsis." *Frontiers in Plant Science* 7 (August 17, 2016). https://doi.org/10.3389/fpls.2016.01242.

Tsai, Allen Yi-Lun, Robert McGee, Gillian H Dean, George W Haughn, and Shinichiro Sawa. "Seed Mucilage: Biological Functions and Potential Applications in Biotechnology." *Plant and Cell Physiology* 62, no. 12 (December 1, 2021): 1847–57. https://doi.org/10.1093/pcp/pcab099.

Voulodimos, Athanasios, Nikolaos Doulamis, Anastasios Doulamis, and Eftychios Protopapadakis. "Deep Learning for Computer Vision: A Brief Review." *Computational Intelligence and Neuroscience* 2018, no. 1 (2018): 7068349. https://doi.org/10.1155/2018/7068349.

Wang, Li, Wei Wang, You-Qun Wang, Yang-Yang Liu, Jing-Xin Wang, Xue-Qin Zhang, De Ye, and Li-Qun Chen. "*Arabidopsis* Galacturonosyltransferase (GAUT) 13 and GAUT14 Have Redundant Functions in Pollen Tube Growth." *Molecular Plant* 6, no. 4 (July 1, 2013): 1131–48. https://doi.org/10.1093/mp/sst084.

Weigel, Detlef, and Jane Glazebrook. "Setting Up Arabidopsis Crosses." *Cold Spring Harbor Protocols* 2006, no. 5 (October 1, 2006): pdb.prot4623. https://doi.org/10.1101/pdb.prot4623.

Wolf, Sebastian. "Cell Wall Signaling in Plant Development and Defense." *Annual Review of Plant Biology* 73, no. Volume 73, 2022 (May 20, 2022): 323–53. https://doi.org/10.1146/annurev-arplant-102820-095312.

Xiang, Lirong, Trevor M. Nolan, Yin Bao, Mitch Elmore, Taylor Tuel, Jingyao Gai, Dylan Shah, et al. "Robotic Assay for Drought (RoAD): An Automated Phenotyping System for Brassinosteroid and Drought Responses." *The Plant Journal* 107, no. 6 (2021): 1837–53. https://doi.org/10.1111/tpj.15401.

Yasrab, Robail, Jonathan A. Atkinson, Darren M. Wells, Andrew P. French, Tony P. Pridmore, and Michael P. Pound. "RootNav 2.0: Deep Learning for Automatic Navigation of Complex Plant Root Architectures." *GigaScience* 8, no. 11 (November 8, 2019): giz123. https://doi.org/10.1093/gigascience/giz123.

Yu, Yongqiang, Wenxin Tang, Wenwei Lin, Wei Li, Xiang Zhou, Ying Li, Rong Chen, et al. "ABLs and TMKs Are Co-Receptors for Extracellular Auxin." *Cell* 186, no. 25 (December 7, 2023): 5457-5471.e17. https://doi.org/10.1016/j.cell.2023.10.017.

FIGURES

A

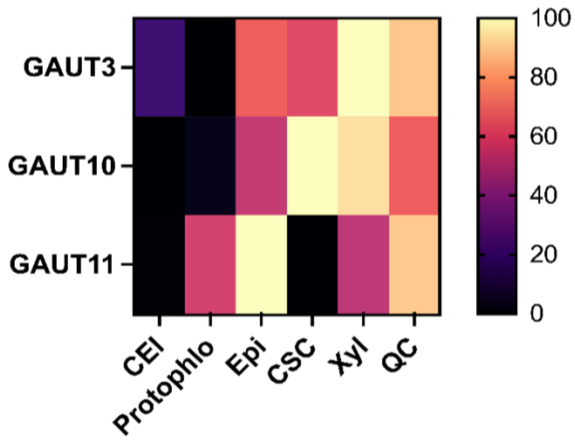

B

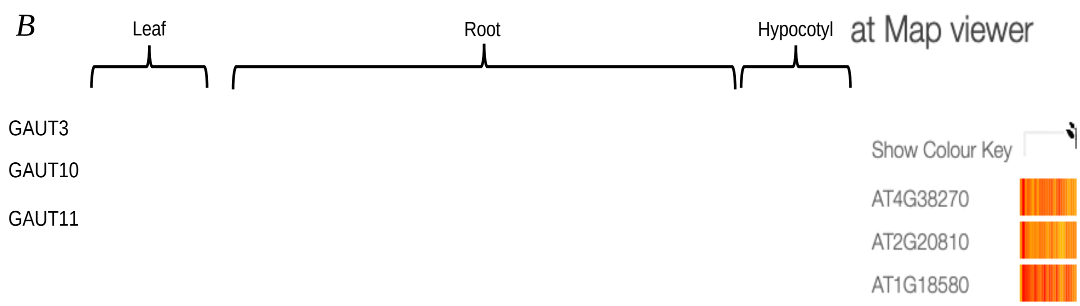

Figure 1. Expression data for *GAUT3, GAUT10,* and *GAUT11* in Arabidopsis.

(A) Transcript abundance of *GAUT3*, *GAUT10,* and *GAUT11* in root apical meristem (RAM) cell types: columella endodermal initials (CEI), protophloem (Protophlo), epidermis (Epi), columella stem cells (CSC), xylem (Xyl), and quiescent center (QC). Expression data from Clark et al., 2019. (B) Transcript abundance of GAUT3, GAUT10, and GAUT11 in leaf tissues (including guard cells), root tissues, and hypocotyls. Expression data from BAR ePlant.

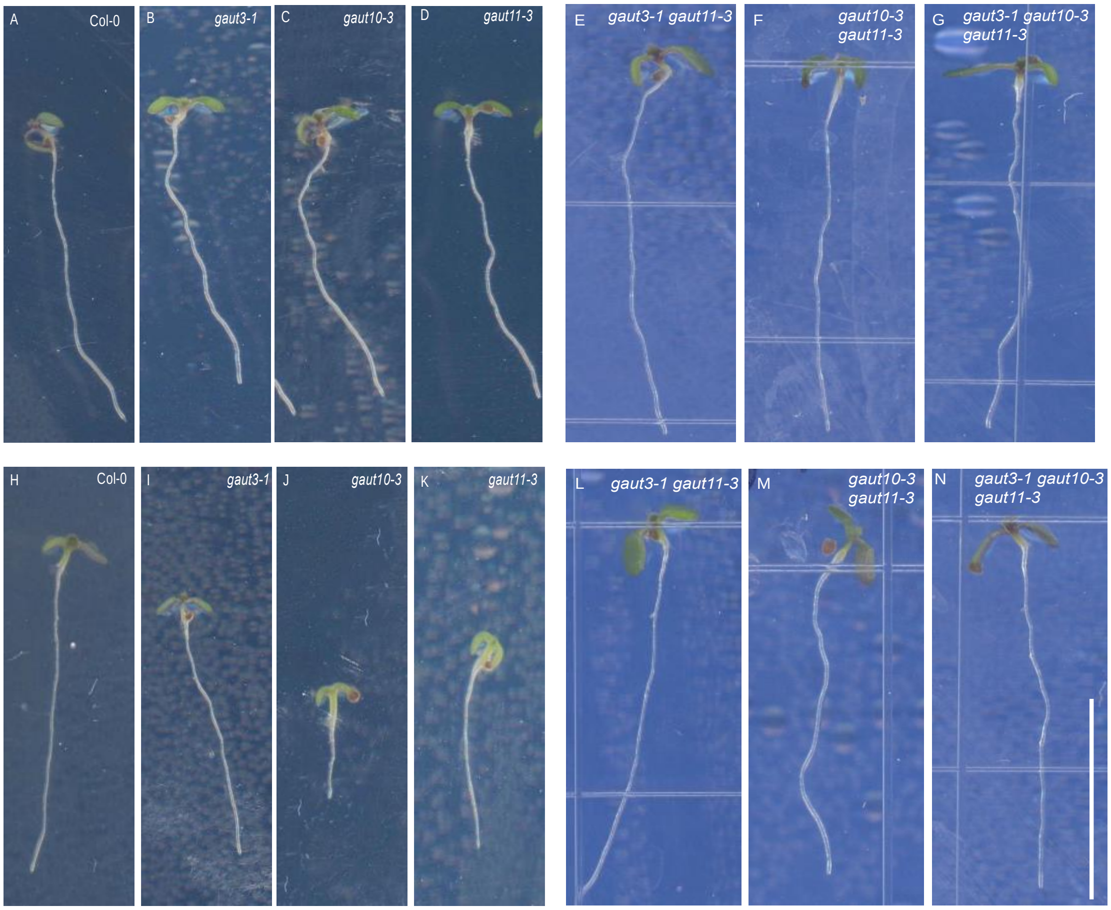

Figure 2. Representative images of *gaut* seedlings.

(A-G) Five-day-old (5 DO) *Arabidopsis thaliana* seedlings grown on 0.5X Linsmaier and Skoog (LS) plates with 0.5% sucrose. (H-N) 5DO seedlings grown on 0.5X LS plates without sucrose. (A,H) Col-0. (B,I) *gaut 3-1* (C,J) *gaut10-3* (D,K) *gaut11-3* (E,L) *gaut3-1 gaut11-3* (F,M) *gaut10-3 gaut11-3* (G,N) *gaut3-1 gaut10-3 gaut11-3*. Scale bar = 1 cm.

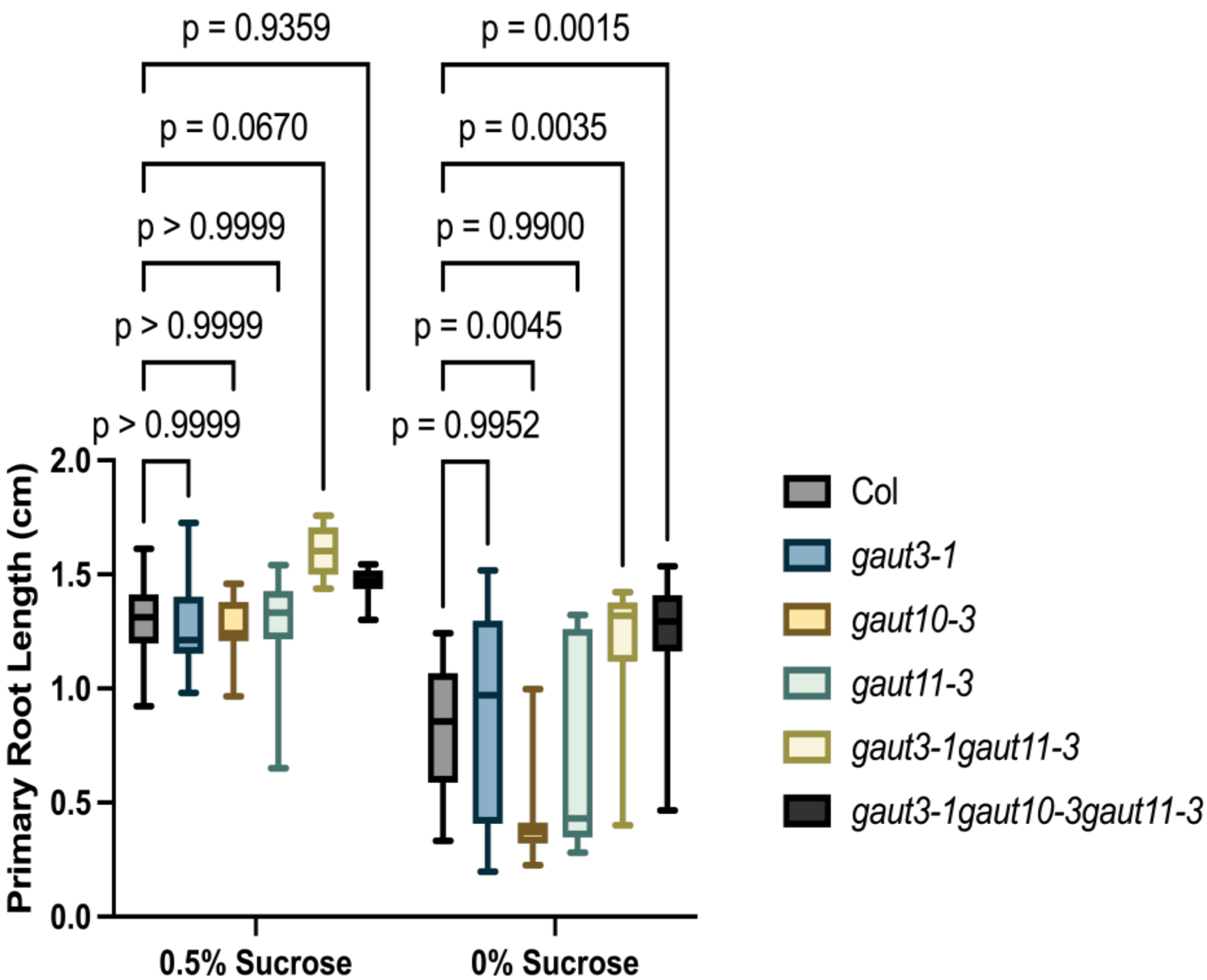

Figure 3. Primary root length of *gaut* seedlings.

Primary root length of five-day-old seedlings grown on 0.5X Linsmaier and Skoog media supplemented with or without sucrose. Statistical significance determined by two-way ANOVA; *P* values for each comparison are shown; values ≤ 0.05 are considered significant.

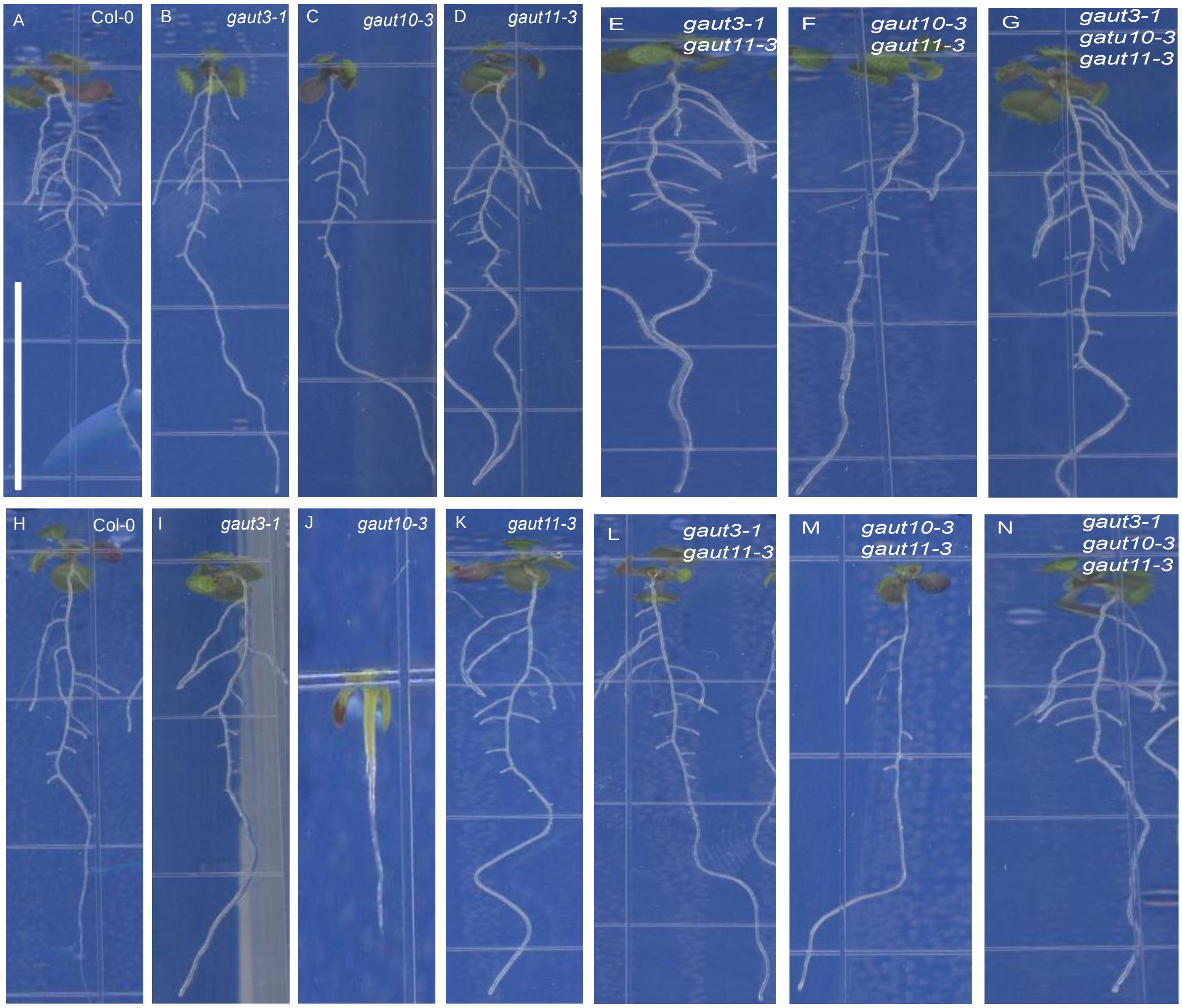

Figure 4. Representative images of *gaut* seedlings with lateral roots.

(A-G) Ten-day-old (10 DO) *Arabidopsis thaliana* seedlings grown on 0.5X Linsmaier and Skoog (LS) media supplemented with 0.5% sucrose (H-N) 10 DO *Arabidopsis thaliana* seedlings grown on 0.5X LS media without sucrose (A,H) Col-0 (B,I) *gaut3-1* (C,J) *gaut10-3* (D,K) *gaut11-3* (E,L) *gaut3-1 gaut11-3* (F,M) *gaut10-3 gaut11-3* (G,N) *gaut3-1 gaut10-3 gaut11-3*. Scale bar = 1 cm.

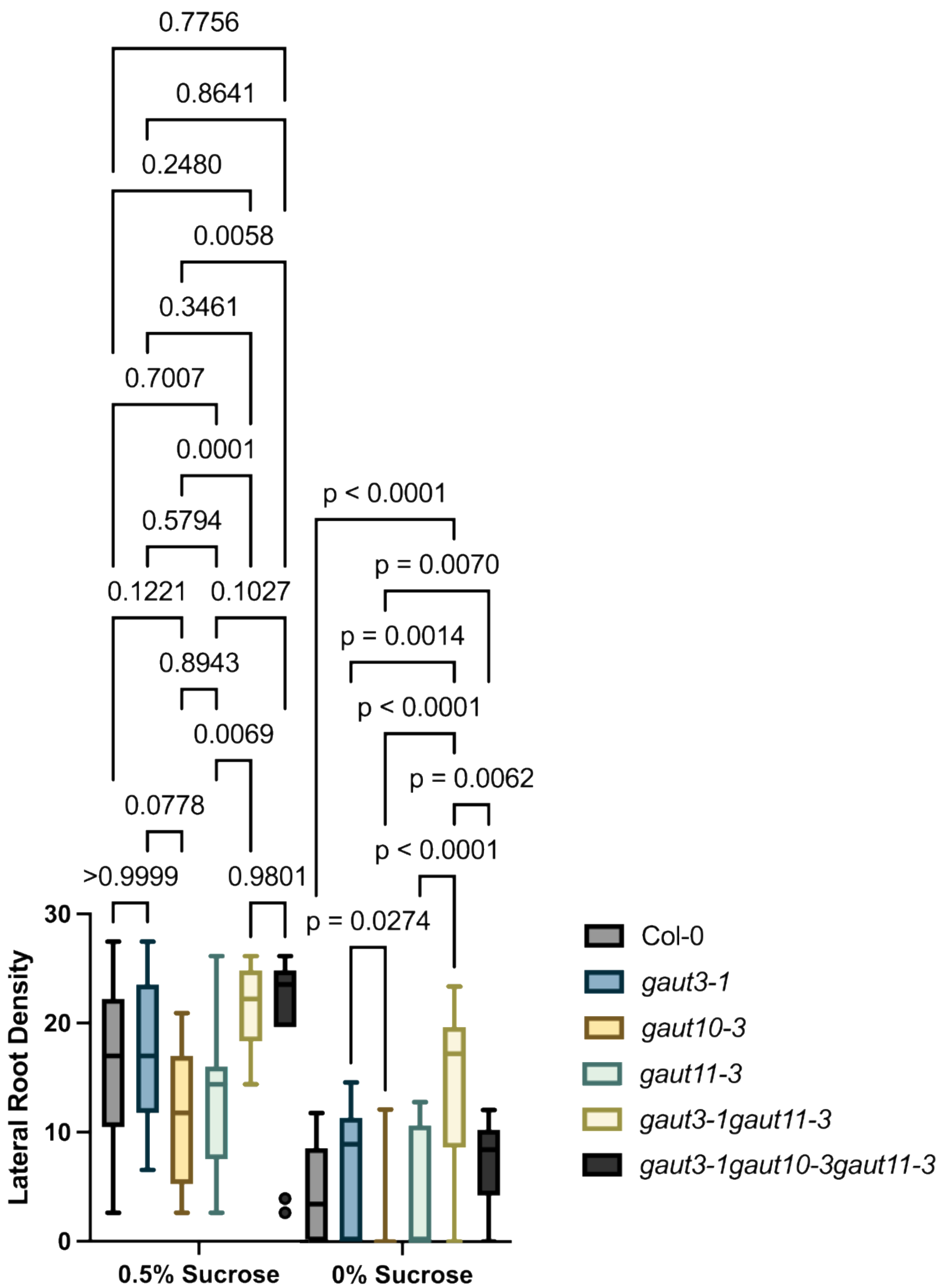

Figure 5. Quantification of lateral root density in *gaut* seedlings.

Lateral root density was calculated for each genotype by dividing the total number of lateral roots by the primary root length for each 10-day-old seedling. Seedlings were grown on 0.5X Linsmaier and Skoog media supplemented with or without 0.5% sucrose. *P* values are from two-way ANOVA to assess statistical significance.

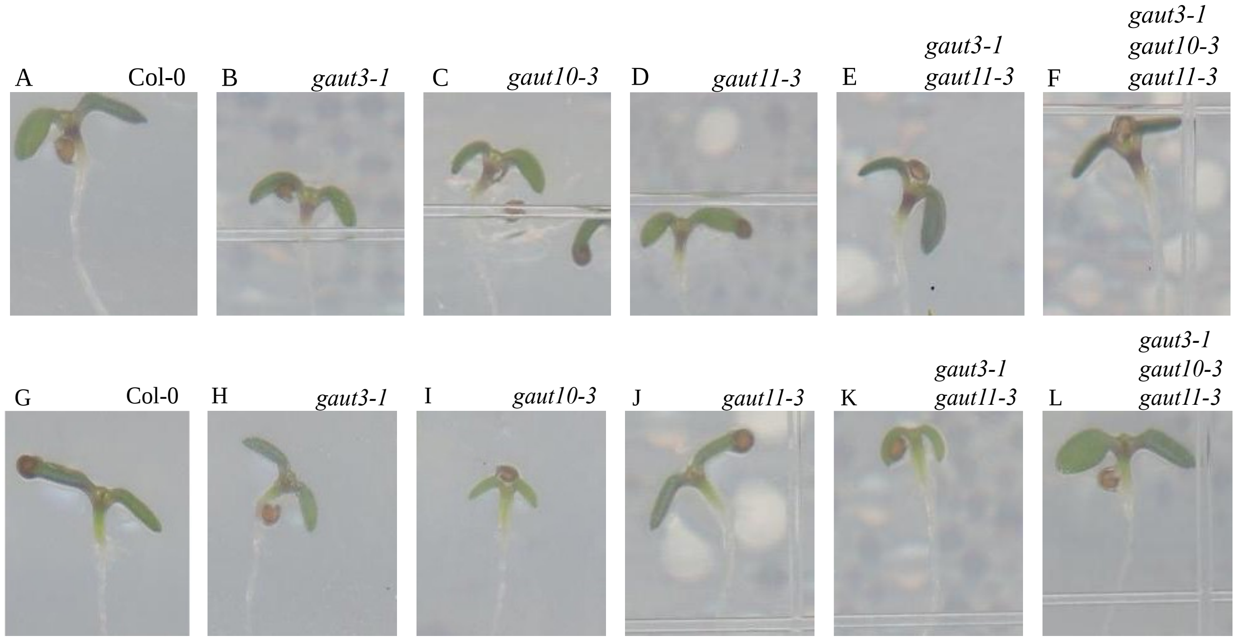

Figure 6. Representative images of light grown 5-day-old hypocotyls.

(A-F) Seedlings were grown on 0.5X Linsmaier and Skoog (LS) media supplemented with 0.5% sucrose. (G-L) Seedlings were grown on 0.5X LS media without sucrose. (A,G) Col-0 (B,H) *gaut3-1* (C,I) *gaut10-3* (D,J) *gaut11-3* (E,K) *gaut3-1 gaut11-3* (F,L) *gaut3-1 gaut10-3 gaut11-3*.

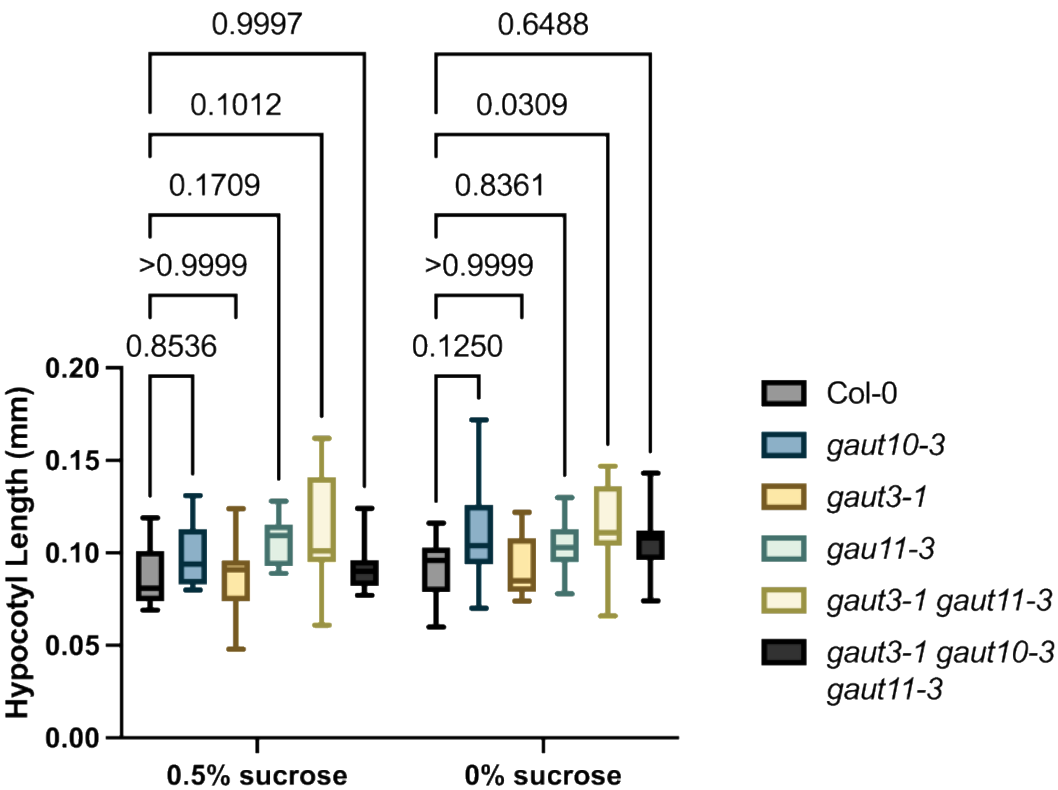

Figure 7. Hypocotyl lengths of 5-day-old *gaut* seedlings.

Hypocotyl lengths were measured using ImageJ/Fiji for each genotype shown grown on 0.5X Linsmaier and Skoog media supplemented with or without 0.5% sucrose. *P* values are from two-way ANOVA to assess statistical significance.

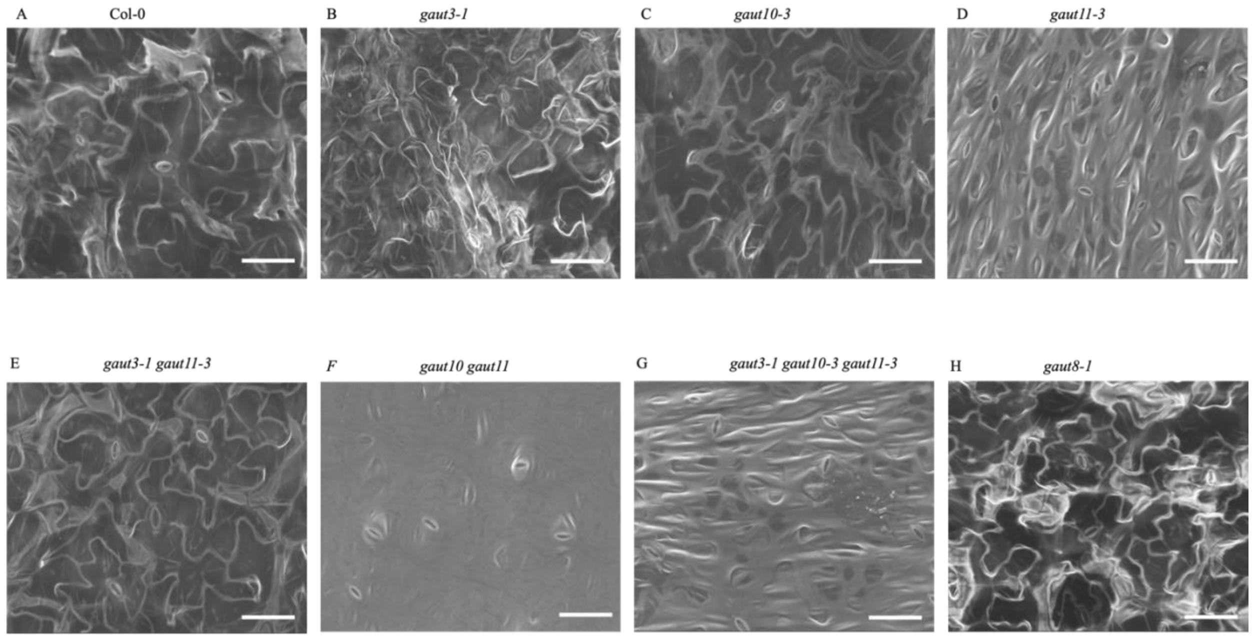

Figure 8. Representative images of 4-week-old abaxial leaf surfaces.

Scanning electron micrographs of abaxial leaf surfaces of soil-grown *Arabidopsis thaliana* genotypes. (A) Col-0 (B) *gaut3-1* (C) *gaut10-3* (D) *gaut11-3* (E) *gaut3-1 gaut11-3* (F) *gaut10-3 gaut11-3* (G) *gaut3-1 gaut10-3 gaut 11-3* (H) *gaut8-1*. Scale bar = 50µm

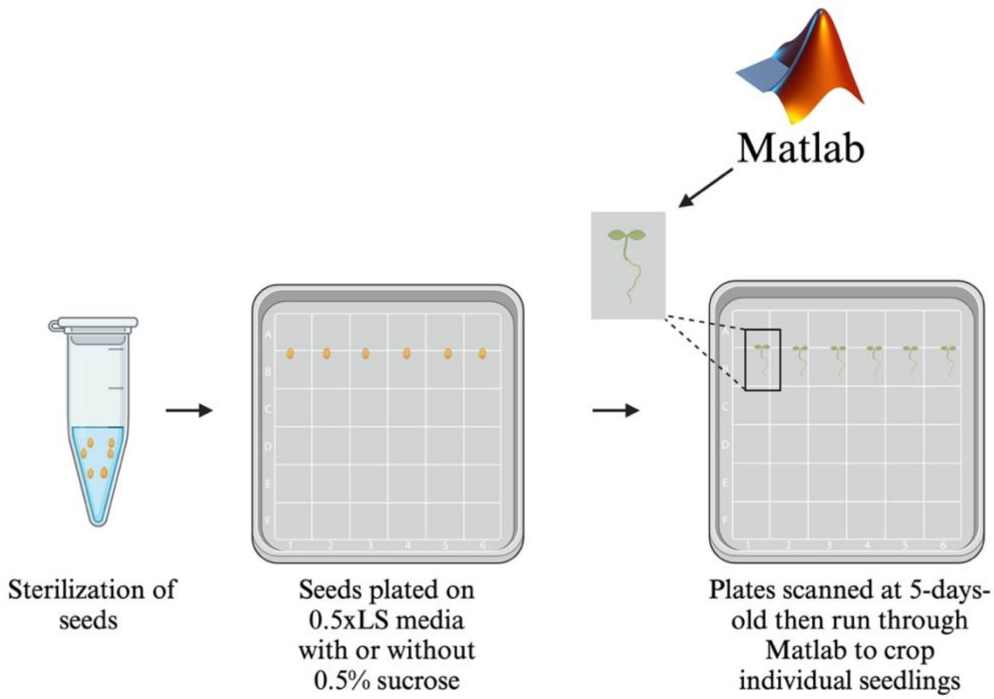

Figure 9. Overview of seed to seedling image.

Seeds in a 1.5ml Eppendorf tube are sterilized with a 1% bleach solution then washed with water five times. Then are plated on 0.5xLS media with or without 0.5% sucrose, at 5-days-old the plates are imaged. Using a MATLAB code designed by Laura Zinnel, can semi-automatically crop selected sections/seedlings. Created in BioRender.com

TABLES

Table 1. Desired mutant combinations of *GAUT* alleles of interest.

Mutant Combinations	**Genotypes**
Single	*gaut3-1* (SALK_001920) *gaut8-1* (SALK_030075) *gaut10-3* (SALK_092577) *gaut11-3* (SAIL_567_H05)
Double mutants	*gaut3-1 gaut10-3* *gaut3-1 gaut11-3* *gaut10-3 gaut11-3*
Triple mutant	*gaut3-1 gaut10-3 gaut11-3* *gaut8-1 gaut10-3 gaut11-3* *gaut3-1 gaut8-1 gaut10-3* *gaut3-1 gaut8-1 gaut11-3*
Quadruple mutant	*gaut3-1 gaut8-1 gaut10-3 gaut11-3*

Table 2. Primers for genotyping Arabidopsis *GAUT* alleles.

Primers	**Sequence (5'-3')**	**Annealing Temperature (C°)**	**Allele**	**Expected Size**
DK905 + DK906	AGAGTCTTGCAGCTGCTTGAG TTTGCAGCGAAGAGAAAGAAG	60	*GAUT10*	~1128bp
DK828 + DK906	ATTTTGCCGATTTCGGAAC TTTGCAGCGAAGAGAAAGAAG	60	*gaut10-3*	~650bp
DK1819 + DK1820	TTTGAAAACTCAGTCATAGGGAAATA GAAGGATGATTTGCTTTGAAATAGTA	59	*GAUT3*	~897bp
DK828 + DK1820	ATTTTGCCGATTTCGGAAC GAAGGATGATTTGCTTTGAAATAGTA	59	*gaut3-1*	~650bp
DK1824 + DK1825	CAACCAATTGCCCAAATATTG GAAAACCCGAAAGGAGAAAAG	60	*GAUT11*	~1020bp
DK1425 + DK1825	TAGCATCTGAATTTCATAACCAATCTCGATACAC GAAAACCCGAAAGGAGAAAAG	59	*gaut11-3*	~300bp

Table 3. *GAUT* alleles used in this study.

Allele	**Stock line**	**Reference**
gaut3-1	SALK_001920	Caffall et al., 2009
gaut3-2	SALK_113167	Caffall et al., 2009
gaut10-3	SALK_092577	Caffall et al., 2009; Pu et al., 2019; Dash et al., 2023
gaut11-3	SAIL_567_H05	Caffall et al., 2009; Guo et al., 2021

Table 4. Summary table of *gaut* phenotypes relative to wild-type Col-0 control**.** “Normal” designates a wild-type phenotype.

Genotype	**Primary root**	**LRD**	**Hypocotyl**
gaut3-1	Normal	Normal	Normal
gaut10-3	Short	Reduced	Normal
gaut11-3	Normal	Normal	Normal
gaut3-1 gaut11-3	Long	Increased	Long
gaut10-3 gaut11-3	Short	Reduced	Short
gaut3-1 gaut10-3 gaut11-3	Long	Normal	Normal